


 Cite this: *RSC Adv.*, 2022, 12, 20403

Study on the anhydrous condensation of collagen polypeptide and tricyanogen chloride

Donglei Liu, Jiaying Zhang, Chuanrui You, Hui Chen * and Zhihua Shan *

The molecular weight of collagen-degrading polypeptides (CDPs) extracted using the alkali method from leather scraps must be expanded to improve its utilization effect. A novel polymer (CPP) was synthesized from tricyanogen chloride (TC) and CDP by mechanical force without water. According to the solution viscosity and content of water-soluble matter, the optimal condensation conditions of the $n(\text{TC})/n(\text{CDP})$ and temperature were obtained and the properties of CPP, such as the molecular weight, thermal properties, and isoelectric point were tested and analyzed. The synthesis of CPP was simulated by the substitution of L-threonine containing hydroxyl and amino groups for the condensation reaction of CDP and TC. The result illustrated that only amino groups were involved in the substitution of chlorine accomplished by the SN₂ pathway. Based on this, a probable formation mechanism of CPP was proposed. As an illustration, CPP has good utilization values in the preparation of a corrugated paper jelly instead of gelatin. The preparation of polypeptide water-based adhesive by a mechanochemical method not only has good controllability in the production process but also can save water and energy.

 Received 1st April 2022
 Accepted 11th June 2022

DOI: 10.1039/d2ra02111k

rsc.li/rsc-advances

1. Introduction

Leather manufacturing is a traditional industry that is beneficial to the economic development of agriculture and animal husbandry, but it is also accompanied by high pollution output.¹ In China, almost 300 000 tons of chromium-containing leather scraps are generated by the leather industry each year.² These chromium-containing leather scraps contain 3.5–4.0% Cr₂O₃ and more than 90% collagen (on a dry basis). However, it is extremely difficult to extract primordial collagen *via* chemical methods from chromium-containing leather scraps because collagen and chromium bind firmly through coordination bonds.^{3,4} However, there are many chemical and biochemical methods for extracting the collagen degradation products, such as industrial gelatin and polypeptide, from leather scraps.^{5–7} These collagen degradation products have been widely used as an industrial intermediate or agricultural organic fertilizer.^{8–10} Among these methods, the alkaline treatment of leather scraps to obtain collagen has been one of the most commonly used methods.⁶ When leather scraps were immersed in a concentration of 20% to 25% lime liquid over 48 h at approximately 25 °C, higher molecular weight gelatin was made available,¹¹ but a great deal of lime sludge and chrome-containing wastewater was discharged. To meet the current environmental requirements, the modern industrial treatment requires a short time and low sewage discharge with strong alkaline chemicals at

higher temperatures to treat the leather scraps. Nevertheless, due to the effect of alkalinity and higher temperature, the peptide bonds of collagen molecules are hydrolyzed considerably. The result is that collagen degradant products with a smaller molecular weight and lower viscosity are obtained.¹²

The quality of the collagen degradation products from collagen can be mainly characterized by its molecular weight, color, and solution rheological properties. The average molecular weight (M_n) of gelatin above 20 000 is an important indicator of industrial gelatin with necessary physical and chemical characteristics for industrial applications. Lower molecular weight polypeptides make their solution less viscous and lose many applications. In terms of theory and practice, cross-linking and branchification of polypeptides can increase the molecular weight and solution viscosity increase when using formaldehyde or epoxides as a crosslinking agent,^{13,14} as well as the use-value of collagen polypeptide can be restored or improved.^{15,16} However, since collagen polypeptide is a macromolecular water-based electrolyte, the reaction of increasing molecular weight makes stirring difficult and the product makes filling barrels and packing difficult. Commonly used protein crosslinkers, such as formaldehyde or epoxides still have a hidden danger of the free monomers.¹⁷

An anhydrous reaction method can directly obtain dry products, which can be considered to be an acceptable method with simple operation and high efficiency.^{19,20} The powdered or granular dry material is considered to have the advantages of a long storage life and convenient transportation.¹⁸ The anhydrous reaction method requires that the reactants can be dispersed effectively in the absence of water or solvent and that

National Engineering Laboratory for Clean Technology of Leather Manufacture, Sichuan University, Chengdu 610000, China. E-mail: scushanzhuhua@163.com; chenh@scu.edu.cn



the degree of homogenization of products becomes the key to the reaction and product quality.²⁰ The purpose of this study is to prepare a new type of high molecular weight gelatin from the collagen degradation products using the mechanochemical method in an anhydrous state. It was found that when the powder of low molecular weight collagen polypeptide extracted from the leather scrap was mixed with melamine, the reaction increasing the molecular weight can be completed by applying heat and mechanical force. The synthetic product provides the possibility of producing new materials for potential biomedical applications. Finally, the synthetic product is prepared into a corrugated adhesive for the application.

2. Experimental materials and methods

2.1. Materials

The chromium-containing leather scraps used in this study were from a leather factory in Hebei, China. Tricyanogen chloride (TC), called 2,4,6-trichlorine-1,3,5-triazine, with a molecular weight of 184.14, was obtained from the Wengjiang Chemical Reagent Co. Ltd. in Guangdong, China. TC is soluble in acetone but has slight solubility in water and three chlorine atoms on it can be replaced in different temperature scopes (0–5 °C, 40–50 °C, 80–90 °C respectively) by sulfhydryl, hydroxyl, and amido groups. Gelatin (AR) is from the Chengdu Kelong Co. Ltd., China.

The complete set of equipment for preparing powdered collagen degradants was from the Liaonin Dacheng Biotechnology Co., Ltd., China. The RE-52CS rotary separator was from the Shanghai Xiande Experimental Instrument Co., Ltd., China. The NDJ-8SN rotary viscometer was from the Shanghai Precision and Scientific Instrument Co., Ltd., China. The gel permeation chromatography (GPC) system was from Dongcao Co., Ltd. The EA 3000 elemental analyzer, was from Leeman Labs Inc. The JSM-7500F scanning electron microscope was from the JEOL Co., Ltd. The IS10 FT-IR spectrometer was from Thermo Fisher Scientific, US. The 200PC DSC analyzer and 209F1 TG analyzer were from the NETZSCH Co., Ltd. The Zeta PAL-type laser particle size analyzer was from Malvern Instruments, UK.

2.2. Prepared powdered collagen degradant product

Leather scraps, containing a moisture content of 50–53%, were added to the reactor, and then, 200% water, 4% lime (50 wt% of calcium oxide), and 3% sodium hydroxide were added, followed by degradation for 4 h at 90 °C. The liquid produced after degradation was filtered under 6 MPa pressure and 500 mesh in a plate and frame filter press. The filtered liquor was neutralized



Fig. 1 Rotary evaporator for preparing CPP.

with ammonium sulfate to a pH of 6.5–7.0. After the compounds of calcium and chromium were separated and the liquid was decolorized by the adsorption of activated carbon, the collagen degradation liquor was filtered again under the 6 MPa pressure and 500 mesh in a plate and frame filter press. The collagen degradation liquor with a solid content of 37.0–38.0% and 0.31–0.33 Pa s viscosity was obtained through vacuum thermal concentration. Finally, the powdered collagen-degraded product (CDP) was obtained after spray drying using a centrifugal spray drier. Some of the key indicators of CDP are shown in Table 1.

2.3. Condensation of CDP and TC

Based on the CDP weight, 3.0–4.0% water, 1.0–3.0% TC, some sodium carbonate, and 100 g glass beads with a diameter of 5 mm were added to a 1000 mL clean and dry round-bottomed flask in a rotary evaporator (Fig. 1) and rotated for 1 h at 2 °C to be mixed uniformly. The mixture was continuously tumbled for 5 h under controlled temperatures of 60 °C, 80 °C, and 100 °C in the same vacuum, and sodium carbonate was added to neutralize the residual HCl. Six kinds of the material ratio $n(\text{TC})/n(\text{CDP})$ (1.0, 1.4, 1.8, 2.2, 2.6, and 3.0) were used in the condensation, and eighteen light yellow powdery regeneration gelatin samples (collagen polypeptide polymers) divided into three groups, called CPP-60, CPP-80, and CPP-100, were obtained. Due to the bleaching effect in the reaction, the appearance color of CPP changed from pale yellow CDP to white CPP.

2.4. Structure and property characterization of CPP

2.4.1. Solubility of CPP. 10.0 g CDP and 10.0 g CPP were suspended in 90.0 g acetone. The unreacted and dissolved tricyanogen chloride in the samples was removed after filtration with 500 nylon gauze on a flat funnel. The gauze solids were washed with 90 g of water in a beaker, and CDP and CPP were further dissolved in water, and centrifugation for 10 min was

Table 1 Some key indicators of CDP

| Appearance | Solubility (25 °C)/% | w(solid)/% | w(ash)/% | M_n | w(protein)/% | $\rho(\text{Cr})/(\text{mg kg}^{-1})$ | w(H ₂ O)/% |
|---------------------|----------------------|------------|----------|--------------------|--------------|---------------------------------------|-----------------------|
| Light yellow powder | 99.5 | 93.1 | 4.7 | 1.23×10^4 | 87.6 | 18.7 | 6.9 |



used to remove the water-insoluble impurities in CDP and CPP. Purified CDP and CPP were freeze-dried and placed in a dryer for sample analysis. Based on the CDP weight, the solubility of CPP was determined. The experimental error was calculated to be within 0.05 grams for each experiment.

2.4.2. Sample solution viscosity. 10.0 g of purified sample (CPP-60, CPP-80, CPP-100, and CDP), CDP, and gelatin were dissolved in 90.0 g of water at 25. The viscosity of each solution was determined by a number 2 rotors in a rotary viscometer at 60 rpm and 25 °C. The 3D plot of each sample's viscosity is shown.

2.4.3. Sample molecular weights. The molecular weights of all samples, including CPP-60, CPP-80, CPP-100, CDP, and gelatin, were determined using a gel permeation chromatography (GPC) system. The chromatographic conditions were as follows: TSK-GEL G-5000 PW xL column (7.8 mm × 300 mm) and G-3000 PW xL column (7.8 mm × 300 mm), 0.02 mol L⁻¹ KH₂PO₄ as the mobile phase with a pH of 6.0, the flow rate of 0.6 mL min⁻¹, a column temperature of 35 °C, and a sample size of 20 μL.

2.4.4. Nitrogen content testing. The nitrogen contents of CPP and CDP were tested and contrasted by an elemental analyzer. As the nitrogen content of CT is higher than that of CDP, comparing the nitrogen contents of CPP and CDP can lead to the calculation of the composition of CPP.

2.4.5. Elemental analysis. The elemental analysis of the CPP sample was observed by scanning electron microscopy-energy dispersive X-ray analysis (SEM-EDS), and the surface structure of powdered collagen particles was speculated.

2.4.6. Infrared spectrum analysis. The CPP sample was made of a potassium bromide press and scanned from 400 to 4000 cm⁻¹ by an IR spectrometer.

2.4.7. DSC analysis. CPP or CDP (5–10 mg, same weight) was loaded into an aluminum pan and heated in nitrogen at a rate of 10 °C min⁻¹ from 30 to 180 °C with an empty aluminum pan as a reference in a DSC analyzer.

2.4.8. TG analysis. An empty aluminum oxide pan was tested from 50 to 600 °C with a heating rate of 10 °C min⁻¹ and a nitrogen gas flow of 20 mL min⁻¹ for obtaining the baseline. CPP or CDP (5–10 mg) was loaded into an aluminum oxide pan. Then, samples were tested in a TG analyzer by applying the baseline file.

2.4.9. Measurement of isoelectric points. CPP or CDP solutions (0.2–0.5 mg mL⁻¹) with different pH values were tested using a Zeta PALS-type laser particle size analyzer for determining the zeta potential of the samples and the curve to obtain an isoelectric point. According to the test results, the isoelectric point could be found.

2.5. Exploration of the mechanism

2.5.1. Simulated product synthesis. The determination of the basic structure of the products' CPP is the key to understanding the mechanism of the condensation reaction of the CDP and TC. Collagen contains active groups that react with TC, the most important of which are free amino and hydroxyl groups on the side chain. The condensation of L-threonine

containing hydroxyl and amino groups instead of CPP with TC was simulated.^{21,22} The material ratio $n(\text{L-threonine}) : n(\text{TC})$ is 3 : 1 and the reaction rotary evaporator was the same as in Fig. 1. Two reactants were mixed and rotated for 1 h at 20 °C. The mixture was continuously tumbled for 5 h under a controlled temperature of 100 °C in the vacuum. The reaction mechanism was characterized and speculated by NMR and FT-IR analysis of the products.

2.5.2. FTIR analysis of simulated products. The simulated product, L-threonine, and TC samples were made up in a potassium bromide press and scanned from 400 to 4000 cm⁻¹ by an FTIR spectrometer.

2.5.3. ¹³CNMR analysis of simulated products. ¹³C NMR spectra of the simulated product and L-threonine samples were measured on a Bruker AVANCE DRX-600 MHz NMR spectrometer using the mixed solvent of D₂O and DMSO-d₆.

2.5.4. Substitution of SN1 and SN2. In addition to the structure of the simulated product to determine whether the substitution reaction is SN1 or SN2, the process of replacing three chlorine atoms in the TC can also determine the reaction mechanism. During the anhydrous synthesis of CPP, if the chlorine is left alone (SN1) the formed Cl₂ can be vacuum-extracted into 10% potassium iodide solution, and then the expression was further carried out with a starch solution.

2.6. Exploration of the functional exploration of CPP-100-2.2

With the rapid development of the logistics industry and the need for a convenient life, corrugated paper is one of the largest quantities of packaging materials in the world. At the same time, corrugated cardboard adhesive has become the most needed adhesive, and China needs nearly 400 000 tons of it each year of 26 million tons of corrugated boards. The main raw materials used for corrugated cardboard adhesives are gelatin-based solid glue containing 40% water, which is required to have several necessary quality indicators, such as high bonding strength in a wide range of relative humidity, excellent initial viscosity between 50–60 °C and low cost. Therefore, industrial gelatin is the most important component of corrugated cardboard adhesive. Because the quality of corrugated paper or sizing operation is required, the adhesive is taken as a solid jelly in its product form.

To prove the application value of the CPP-100-2.2 product, CPP-100-2.2-based corrugated cardboard adhesive was studied, for which the initial viscosity, bonding strength, and water-resistance indices were explored.

2.6.1. Preparation of solid gelatum. Based on the weight of CPP-100-2.2, 95% distilled water, 5% glucose, and an appropriate amount of xanthan gum were mixed with CPP-100-2.2. After stirring for 5–7 h at 75–80 °C, the corrugated cardboard adhesive, called CPP-G (50 wt%) was prepared. The viscosity of the CPP-G was measured at 50 °C after being stored for one day.

2.6.2. Initial adhesion of CPP-G. Pieces of clean corrugated fiber paper that were 12 cm × 10 cm were used. The square-shaped area in each paper, which was approximately 10 cm on a side, was divided into 100 the same square-shaped areas. The square-shaped areas of the two-shaped papers were stuck



together rapidly (in opposite directions) after one square-shaped area was coated with 2 g of CPP-G at 50 °C. According to the separation operation, after two minutes of the bonding, the initial adhesion of CPP-G as the ratio of the damaged area to the total area was obtained. This experiment was repeated 3 times, and the data were averaged.

2.6.3. Bonding strength of CPP-G. A paper board was cut into 5 cm × 2 cm strips. Similarly, the square-shaped areas of approximately 2 cm on a side of the two-shaped papers were stuck together rapidly after one square-shaped area was coated by 0.08 g of CPP-G at 50 °C. Ten minutes later after drying, the papers were tested using a horizontal testing machine at a drawing speed of 10 mm min⁻¹, and the ratio of the minimum breaking force was calculated to be 4 cm² for coated CPP-G, upon which the bonding strength of CPP-G was calculated. The experiment was repeated 3 times, and the data were averaged.

2.6.4. Water-resistance of fiberboard adhered by CPP-G. According to the corrugated fiberboard determination of the water-resistance of the glub bond (immersion),²³ corrugated fiberboard adhered by CPPG was suspended in water. The period of time from the suspension in water to the paper board and core naturally separating was represented by the water resistance of CPPG.

3. Experimental results and discussion

The simulated condensation process and product are shown in Fig. 2. At each temperature, one to three chlorine atoms of tri-cyanogen chloride may be substituted and bound to collagen polypeptides in the form of a single point, which led to the differences in the physical and chemical properties between the CPP and the CDP. Although the reaction temperature exceeds 80 °C, three chlorines in the TC molecule can be completely replaced in solution, the process is not easy without the action of water.

3.1. CPP product optimization selection

3.1.1. Solubility and viscosity of CPP products

3.1.1.1 Solubility results. According to the results of the dissolution experiment in Section 2.4.1, the solubility of all

Table 2 The solubility of the products and condensation conditions

| Product | Solubility (%) at $n(\text{TC})/n(\text{CDP})$ | | | | | |
|---------|--|------|------|------|------|------|
| | 1.0 | 1.4 | 1.8 | 2.2 | 2.6 | 3.0 |
| CPP-60 | 97.0 | 96.0 | 95.0 | 95.0 | 93.0 | 92.0 |
| CPP-80 | 95.0 | 96.0 | 96.0 | 95.0 | 94.0 | 93.0 |
| CPP-100 | 98.0 | 98.0 | 97.0 | 97.0 | 90.0 | 84.0 |

products was tested and is shown in Table 2. When the ratio was below 2.2, there was no clear correlation between temperature and solubility. However, when the ratio ≥ 2.2 , as the temperature and ratio of condensation were increased, or hydrophobicity increased with increasing molecular weight, the soluble matter was decreased,²⁴ which was thought to be due to the formation of a small amount of the macromolecular gel and then was separated when CPP was filtered with water and centrifuged.

3.1.1.2 Viscosity analysis. As is well known, the solution viscosity is related to the molecular weight and structures of protein macromolecules at the same concentration, temperature, and pH. A high solution viscosity can be considered when the products have a high molecular weight. The relationship between the solution viscosity, condensation temperature, and constituent ratio $n(\text{TC})/n(\text{CDP})$ is expressed in Fig. 3. Because a higher temperature made the chlorine atoms on CT have higher activity, the multipoint binding of CT was easily formed by replacing chlorine atoms with amino groups of the peptide chains. Analogously, at the same temperature, the higher the amount of TC is, the higher the chlorine atom activity is and the greater the chance of cross-linking with the CDP chain. Upon varying the $n(\text{TC})/n(\text{CDP})$ from 1.0 to 3.0 and temperature from 60 °C to 100 °C, the solution viscosity of CPP increased from 0.256 Pa s to 0.418 Pa s, and the solution viscosities of products are shown in Fig. 3. The maximum solution viscosity of CPP was 0.418 Pa s (CPP-100, $n(\text{TC})/n(\text{CDP}) = 3.0$), which is two times larger than that of CDP, which proved that the dry condensation of CDP is effective in increasing the viscosity of CPP solutions. However, when the $n(\text{TC})/n(\text{CDP}) = 2.6$ and 3.0 at 100 °C, the solubility of the product decreased rapidly because of the insoluble gel, which is shown in Table 2. The condensation conditions for high solubility (97%) are $n(\text{TC})/n(\text{CDP}) = 2.2$ and

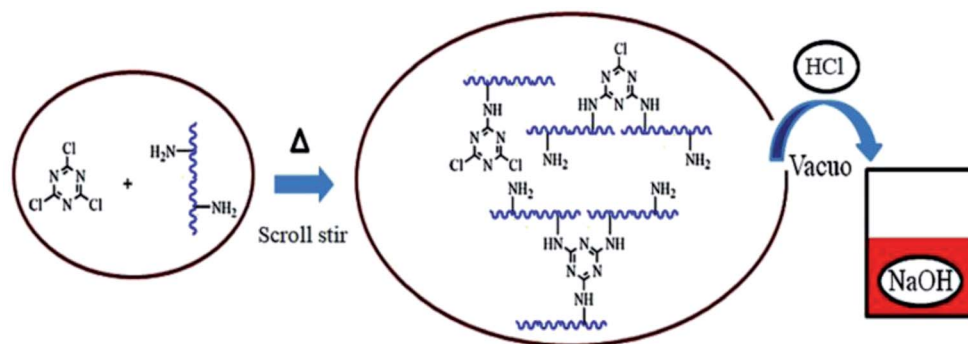


Fig. 2 Collagen polypeptide condensation reaction.



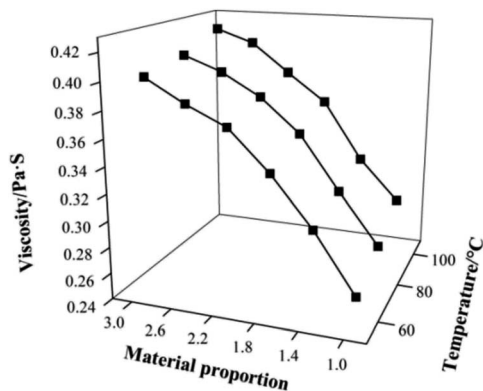


Fig. 3 CPP viscosity and condensation conditions.

Table 3 Viscosity contrast of 10% solution of samples

| Sample | CDP | Gelatin | CPP-100-2.2 |
|------------------|-------|---------|-------------|
| Viscosity (Pa s) | 0.203 | 0.405 | 0.408 |

100 °C, and these are also the closest to gelatin solution viscosity. The ideal condensation product was CPP-100-2.2. The solution viscosities of three samples (CDP, gelatin, and ideal product) are shown in Table 3.

3.2. Characterization of product CPP-100-2.2

3.2.1. Molecular weight of CPP-100-2.2. GPC was used to test the relative molecular weights of CPP-100-2.2, CDP, and gelatin (Fig. 4).

Generally, a larger molecule passes more quickly than a smaller molecule under the same elution conditions when the mixtures are examined on the chromatographic column. The CPP-100-2.2 took less time to make it through the column, and thus, it can be estimated that the molecular weight of CPP-100-2.2 is larger than that of CDP and gelatin.

Table 4 shows that the weight average molecular weight (M_w) values of CDP, CPP-100-2.2, and gelatin are 1.23×10^4 , 6.18×10^4 , and 5.20×10^4 , respectively. When $n(\text{TC})/n(\text{CDP}) = 2.2$, the

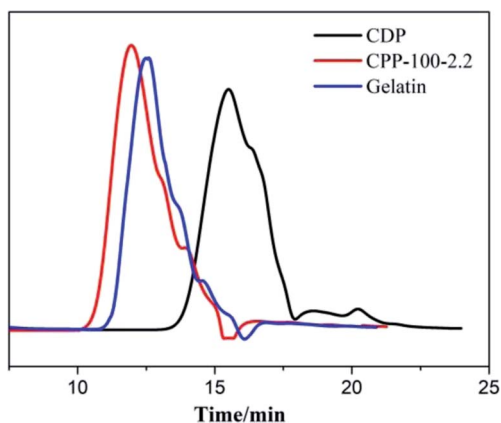


Fig. 4 GPC elution time.

Table 4 GPC analysis of samples

| Sample | M_w | M_n | D |
|-------------|--------------------|--------------------|-------|
| CDP | 1.23×10^4 | 4.99×10^3 | 3.459 |
| CPP-100-2.2 | 6.18×10^4 | 2.39×10^4 | 2.586 |
| Gelatin | 5.20×10^4 | 2.72×10^4 | 1.901 |

connection of TC with CDP enlarged the molecules and made the M_w of CPP-100-2.2 nearly five times that of CDP. It can be seen that although the small molecule polypeptide fragments in CDP can achieve molecular weight increase through cross-linking, the larger molecule polypeptide fragments are more easily crosslinked. However, the number-average molecular weight M_n is still less than that of gelatin. Moreover, Table 4 shows that the polydispersity index of CPP-100-2.2 is 2.586, which indicates that CPP-100-2.2 has lower monodispersity than gelatin.

3.2.2. Nitrogen content of CPP-100-2.2. After testing, the nitrogen content of CPP-100-2.2 was approximately 16.3%, which was higher than that of CDP (approximately 14.8%, based on 87.6% protein content). The increase in the nitrogen content indicated that TC molecules were grafted onto the CDP chains. Thereafter, the grafting yield obtained from theoretical calculations was approximately 5.14%.

3.2.3. Chlorine content of CPP-100-2.2. EDS technology was employed for CDP and CPP-100-2.2. The results illustrate that Fig. 5A gives a clear nickel peak and shows trace amounts of chloride ions in CDP, and Fig. 5B shows that TC was successfully grafted onto the collagen peptide chains to form a product

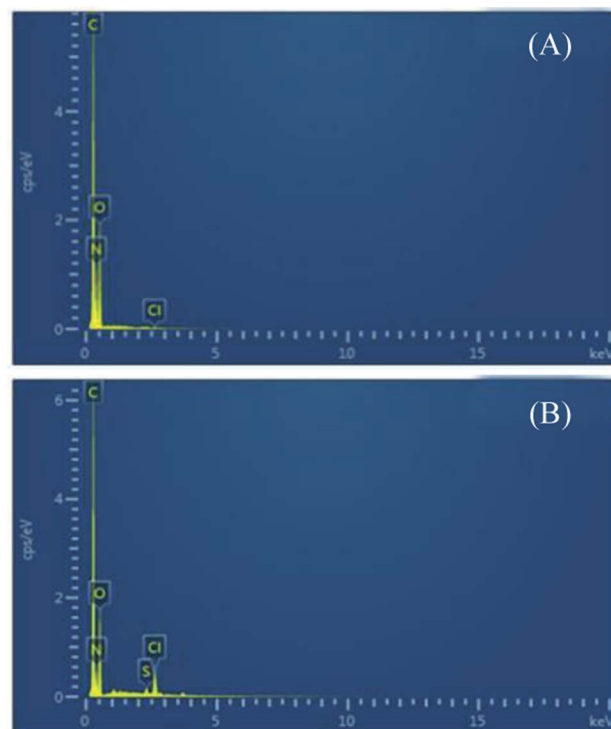


Fig. 5 EDS spectra of samples (A): CDP (B): CPP-100-2.2.



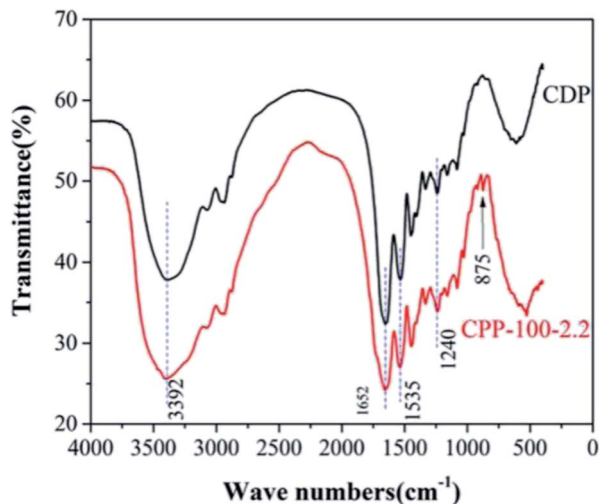


Fig. 6 FT-IR spectra of samples.

CPP-100-2.2 so that the content of chlorine ions increased. At the same time, the increase in chlorine atoms in Fig. 5B also indicates that the three chlorine atoms in TC were not completely replaced despite the good combination of TC and CDP.

3.2.4. FTIR analysis of CPP-100-2.2. The FTIR spectra of CDP and CPP-100-2.2 are shown in Fig. 6. The characteristic absorptions of some groups include that the absorption peak at approximately 1652 cm^{-1} belonging to $\nu(\text{C}=\text{O})$, and $\nu(\text{C}=\text{N})$ is difficult to distinguish. The $\nu(\text{C}-\text{Cl})$ absorption peak at 875 cm^{-1} could be confirmed from the combination of TC and CDP, which means again that the three chlorine atoms in TC have not been completely replaced.

3.2.5. Thermal denaturation of CPP-100-2.2. The DSC curves of CDP and CPP-100-2.2 are presented in Fig. 7. As shown, the thermal denaturalization temperature moved from $85\text{ }^{\circ}\text{C}$ for CDP to $80\text{ }^{\circ}\text{C}$ for CPP-100-2.2. On the one hand, this shows that the binding of TC to CDP resulted in the side chains of polypeptide molecules increasing and the thermal denaturation temperature decreasing, and on the other hand, the decrease in thermal stability of CPP-100-2.2 indicates that the

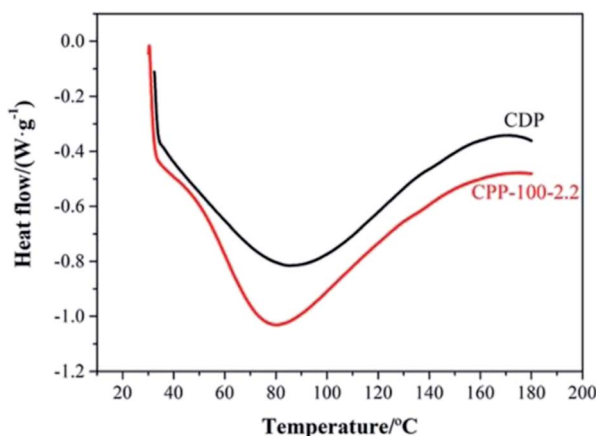


Fig. 7 DSC curve of samples.

TC binding to polypeptide molecules is mainly a simple graft rather than crosslinking.

Regarding the endothermic peak area of the DSC, the melting enthalpy of CPP-100-2.2 was 104.7 J g^{-1} (by integrating the heat absorption peak area), which is larger than the 65.9 J g^{-1} of CDP. The reason was that the destruction of the CPP-100-2.2 structure grafted by CT needs further energy than the chain structure in CDP.

3.2.6. Thermal stability of CPP-100-2.2. The thermal behavior of CDP and CPP-100-2.2 were analyzed by TGA, and the results are shown in Fig. 8. From the thermogravimetric curves in Fig. 8, it can be clearly seen that there are two weight loss processes of CDP, the evaporation process of the moisture and the breakdown process of the polypeptide structure. In contrast, CPP-100-2.2 has a weight loss process at approximately $180\text{ }^{\circ}\text{C}$, which may be the volatilization of unreacted chlorine atoms of TC (over the melting point of $146\text{ }^{\circ}\text{C}$). The departure of chloride ions to obtain new cross-links with collagen peptides resulted in slightly improved thermal stability in the $220\text{ }^{\circ}\text{C}$ to $260\text{ }^{\circ}\text{C}$ range.²⁵ The overall structural stability of CPP is not as good as that of CDP, resulting in a lower maximum weight loss temperature than that of CDP. The final weight loss rate of CPP-100-2.2 was lower than that of CDP as CPP-100-2.2 was having high carbon and chloride contents.

3.2.7. Isoelectric point of CPP-100-2.2. The zeta potential is a quantity for describing the surface charge property of colloidal particles. When the number of positive charges on the surface of the colloidal particles is equal to the number of negative ions adsorbed by the fixed layer, the zeta potential of the colloidal particles becomes zero, meaning that the pH of the solution now corresponds to the isoelectric point. Testing the zeta potentials of CDP and CPP-100-2.2 solutions in pH values of 2.0–9.0, the results are shown in Fig. 9.

From the results in Fig. 9, it can be found that the isoelectric point of CPP-100-2.2 was approximately 5.0, which is smaller than 5.25 of CDP because the amino groups on the peptide

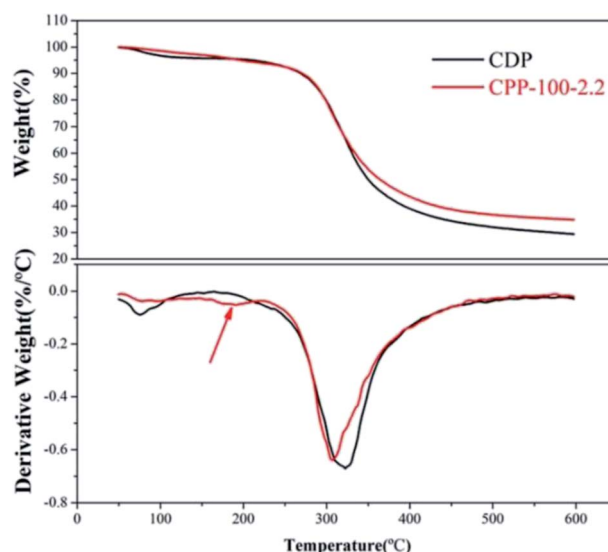


Fig. 8 TGA-DTG spectra of sample before and after reaction.



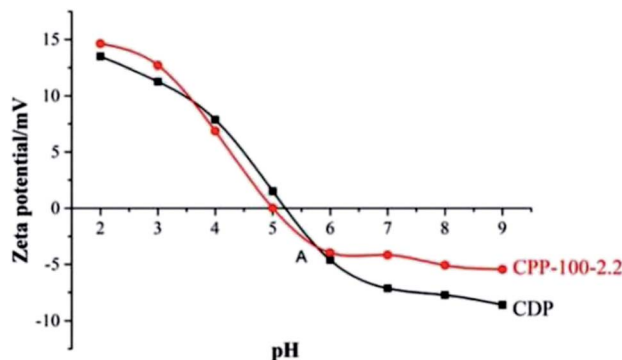


Fig. 9 Zeta potential results of sample.

chains reacted in CPP-100-2.2.²⁵ When the pH is higher than 6, the zeta potential appears constant. It can be understood as each CDP molecule has 4.8 moles of free amino groups (based on $M_n = 12\ 300$), as demonstrated,²⁶ were replaced by TC (based on 5.14% graft rate) and no longer received negative ions or emitted protons.

3.3. Analysis of CPP formation mechanism

3.3.1. FTIR comparative analysis. The FTIR spectra of TC depicted in Fig. 10 illustrate that the stretching vibration $\nu(\text{C}=\text{N})$ appeared at $1496\ \text{cm}^{-1}$. But $\nu(\text{C}=\text{N})$ presents at $1481\ \text{cm}^{-1}$ in the simulated product from the synthesis of L-threonine and TC, which indicates that the chlorine atom of the TC molecule may be replaced by the hydroxyl or amino group of threonine because the energy of $\nu(\text{C}=\text{N})$ is reduced by conjugation. The absorption peak at $1625\ \text{cm}^{-1}$ is ascribed to the stretching vibration $\nu(\text{N}-\text{H})$ of the $-\text{NH}_2$ in L-threonine but it is observed at $1623\ \text{cm}^{-1}$ because the electron cloud on the N atom is reduced because of conjugation. Both threonine and the simulated product have hydroxyl absorption peaks at $900\ \text{cm}^{-1}$. The three vibration peaks above represent substitutions of chlorine on TC molecules involving amino groups of threonine. In addition, the absence of the ether bond (C-O-C) absorption peak in the

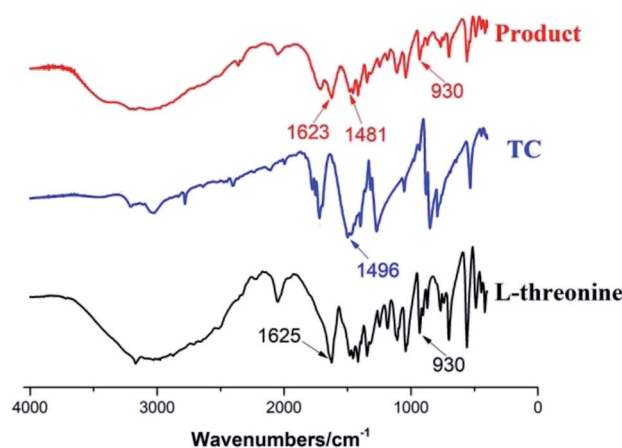
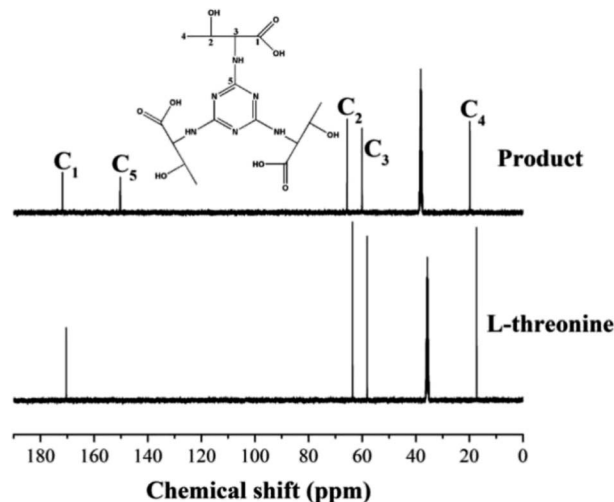


Fig. 10 FTIR spectra of L-threonine, TC and LCPP.

Fig. 11 ^{13}C NMR spectra of L-threonine and LCPP in the mixed solvent.

simulated product also indicates that the hydroxyl group of L-threonine is not involved in the reaction.

3.3.2. ^{13}C NMR analysis. Since L-threonine is insoluble in solvents, D_2O and DMSO, were used. The ^{13}C NMR of the samples was measured to further clarify the structure of the simulated product. In ^{13}C NMR spectra of L-threonine (Fig. 11), the peak at $63.62\ \text{ppm}$ resulted from the carbon atom (C_2) connected by the $-\text{OH}$ group, and the peak at $58.16\ \text{ppm}$ resulted from the carbon atom (C_3) of the $-\text{NH}_2$ group. In addition, the peak at $170.39\ \text{ppm}$ is due to the carboxyl carbon atom (C_1). In the ^{13}C NMR spectra of the simulated product (Fig. 11), the new peak at $150.26\ \text{ppm}$ is attributed to the three carbon atoms (C_5) of the triazine ring, on which all of the chlorine was replaced by one element. In the simulated product, the peak at $65.65\ \text{ppm}$ resulted from C_2 moving by $0.50\ \text{ppm}$ compared to L-threonine and the peak at $60.05\ \text{ppm}$ resulted from C_3 moving by $0.64\ \text{ppm}$. The results showed that only the amino groups of L-threonine were involved in the substitution of chlorine.

3.3.3. The form of substituted chlorine. According to experiment Section 2.5.4, it was found that the drawn-out chlorinated reaction product could not cause discoloration of the potassium iodide solution, which indicates that no chlorine was formed during the formation of CPP products. The formation of CPP was accomplished by the $\text{S}_{\text{N}}2\text{Ar}$ pathway.

3.3.4. Condensation process of CPP. The formation process of CPP can be inferred from the experimental results from Sections 3.3.1 to 3.3.3, as shown in Fig. 12.²⁷

3.4. Characteristics of gelatum CPP-G

The appearance of CPP-G is shown in Fig. 13.

The physical and mechanical indices of corrugated paper bonded with CPP-G at $50\ ^\circ\text{C}$ are shown in Table 5. Compared to commercial adhesive, the adhesive properties of CPP-G were well confirmed. The bonding strength, as a key indicator of corrugated board, meets the national standard (GB/T6544-2008) S-1.1 grade excellent product requirements ($\geq 64\ \text{N cm}^{-2}$). In



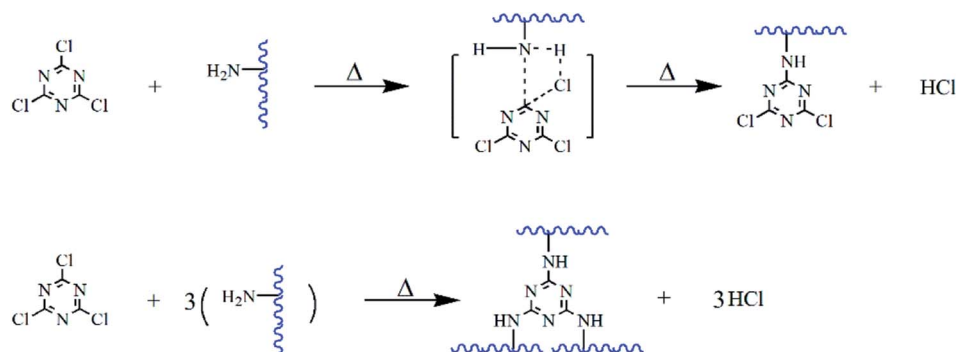


Fig. 12 The formation process of CPP.

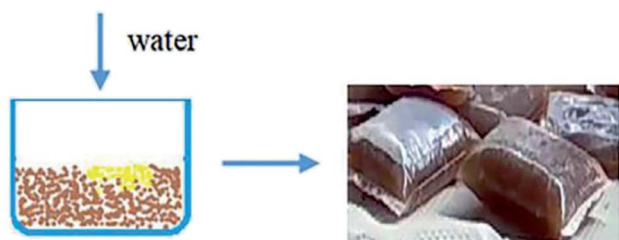


Fig. 13 Appearance of solid jelly CPP-G.

Table 5 Adhesive property of CPP-G

| Sample | Moisture content/% | Viscosity/ Pa s (50 °C) | Initial adhesion/% | Bonding strength/ (N cm ⁻²) | Water resistant time/h |
|---------------------|--------------------|-------------------------------|-----------------------|---|------------------------------|
| CPPG | 35.0 | 9.5 | 90.0 | 79.6 | 48 |
| Commercial adhesive | 35.0 | 10.0 | 95.0 | 80.3 | 48 |

particular, the addition of cyanuric chloride TC cause the crosslinking product CPP-G have water resistance similar to that of commercial glue.

4. Conclusions

The above experiments demonstrated the preparation and functional characterization of the polymer (CPP) by an anhydrous synthesis of collagen degradant product (CDP) and tri-cyanogen chloride (TC). In contrast to gelatin, the condensation conditions selected are $n(\text{TC})/n(\text{CDP}) = 2.2$ and 100 °C, and the product is called CPP-100-2.2, which demonstrated the success of this dry condensation. The condensation replaced CDP with L-threonine illustrated through FT-IR, ¹³CNMR that only amino groups were involved in the substitution of chlorine. A further test was performed for another condensation product hydrogen chloride. All the data show that the condensation reaction was completed through the SN₂ pathway. The CPP-100-2.2 has good value in the preparation of corrugated paper jelly.

As the raw material CDP from the leather scraps, this study meets the requirements of waste recovery in the leather

industry. Furthermore, the preparation of CPP involves an anhydrous condensation reaction without formaldehyde and no waste liquid is discharged, which is a new environmentally-friendly chemical approach.

Conflicts of interest

There are no conflicts to declare.

Acknowledgements

This work was supported by Sichuan Science Technology Program (2019YFG0269).

References

- 1 K. T. W. Alexander, D. R. Corning and N. J. Cory, Environmental and safety issues - clean technology and environmental auditing, *J. Soc. Leather Technol. Chem.*, 1992, **76**(1), 17–23.
- 2 F. Chunqi, J. Xuguang and L. Guojun, Nitrogen-containing gaseous products of chrome-tanned leather shavings during pyrolysis and combustion, *Waste Manag.*, 2018, **78**, 553–558.
- 3 L. F. Cabeza, M. M. Taylor and G. L. DiMaio, Processing of leather waste: pilot scale studies on chrome shavings. Isolation of potentially valuable protein products and chromium, *Waste Manag.*, 1998, **18**(3), 211–218.
- 4 V. G. Pouloupoulou, D. Katakis and E. Vrachnou, A method for the removal of chromium from tanned leather wastes, *J. Air Waste Manag. Assoc.*, 1998, **48**(9), 846–852.
- 5 J. Zarlok, K. Smiechowski and M. Kowalska, Hygienic properties of leather finished with formulations containing collagen hydrolysate obtained by acid hydrolysis, *J. Soc. Leather Technol. Chem.*, 2015, **99**(6), 297–301.
- 6 M. M. Taylor, E. J. Diefendorf and W. N. Marmer, Effect of various alkalinity-inducing agents on chemical and physical properties of protein products isolated from chromium-containing leather waste, *J. Virol.*, 1994, **89**(7), 221–228.
- 7 A. Crispim and M. Mota, Leather shavings treatment - An enzymatic approach, *J. Soc. Leather Technol. Chem.*, 2003, **87**(5), 203–207.



- 8 A. S. Popiolski, R. M. Dallago and J. Steffens, Ultrasound-assisted extraction of Cr from residual tannery leather: Feasibility of ethylenediaminetetraacetic acid as the extraction solution, *ACS Omega*, 2018, **3**(11), 16074–16080.
- 9 F. G. E. Nogueira, I. A. Castro and A. R. R. Bastos, Recycling of solid waste rich in organic nitrogen from leather industry: Mineral nutrition of rice plants, *J. Hazard. Mater.*, 2011, **186**(2–3), 1064–1069.
- 10 L. C. Coelho, M. M. Ferreira and A. R. R. Bastos, Leather Industry Waste as a Nitrogen Source for Wheat and Rice in Succession, *Rev. Bras. Cienc. Solo*, 2015, **39**(5), 1445–1455.
- 11 Y. Fang, Making of gelatin involves cleaning skin of cattle, pigs and other livestock, soaking fur in lime water or sodium sulfide solution, removing fur, dividing large samples of skin into small samples and then soaking in lime water, CN:106433484A, 2017.
- 12 F. Langmaier, P. Mokrejs and K. Kolomaznik, Biodegradable packing materials from hydrolysates of collagen waste proteins, *Waste Manag.*, 2008, **28**(3), 549–556.
- 13 W. Chengwen, M. Renzhou and W. Ruihe, Synthesis and mechanism study of gelatin grafted acetone formaldehyde sulphonates as oil-well cement dispersant, *RSC Adv.*, 2017, **7**(50), 31779–31788.
- 14 L. Yaming, C. Xiao and H. Chuanming, Modified gelatin with quaternary ammonium salts containing epoxide groups, *Chin. Chem. Lett.*, 2014, **8**(25), 1193–1197.
- 15 M. M. Taylor, L. F. Cabeza and W. N. Marmer, Preparation of high molecular weight products by crosslinking protein isolated from the enzymatic processing of chromium containing collagenous waste, *Leather Sci. Eng.*, 2005, **15**(2), 3–5.
- 16 C. Lee and A. Y. Singla, Biomedical applications of collagen, *Int. J. Pharm.*, 2001, **221**(1), 1–22.
- 17 S. Murali, M. Balaraman and R. R. Jonnalagadda, Leather solid waste: An eco-benign raw material for leather chemical preparation - A circular economy example, *Waste Manag.*, 2019, **87**, 357–367.
- 18 Z. Yingfeng, G. Jiyou and Y. Long, Preparation and characterization of dry method esterified starch/poly(lactic acid) composite materials, *Int. J. Biol. Macromol.*, 2014, **64**, 174–180.
- 19 Z. Bing, G. Honghong and L. Shaoyu, Synthesis and characterization of carboxymethyl potato starch and its application in reactive dye printing, *Int. J. Biol. Macromol.*, 2012, **51**(4), 668–674.
- 20 G. Andrew, *New Developments in Waferboard/OSB Resin Technology. Proceedings Twenty-Two International Particle Board Symposium*, WSU, Pullman, 2016, pp. 123–132.
- 21 Z. Yuhan, K. Georgina and K. Maria, A mild and selective method for the catalytic hydrodeoxygenation of cyanurate activated phenols in multiphase continuous flow, *Org. Process Res. Dev.*, 2016, **20**(11), 2012–2018.
- 22 Z. Jialin, H. Yuanhang and H. Jingjing, Synthesis and properties of acetylene-containing cross-linkable triazine resin, *EXPRESS Polym. Lett.*, 2020, **14**(08), 780–792.
- 23 *Corrugated fiberboard-Determination of the water resistance of the glub bond (immersion)*, GB/T10512-2008, China, 2008.
- 24 H. Yamamoto, Y. Hirata and H. Tanisho, Cross-linking and insolubilization studies of water-soluble poly(L-ornithine) Cross-linking and insolubilization studies of water-soluble poly(L-ornithine), *Int. J. Biol. Macromol.*, 1994, **16**(2), 81–85.
- 25 I. Chakarska, I. Goshev, I. Goshev, *et al.*, Cross-linking phosphoric acid hydrolysates. of collagen with cyanuric chloride, *J. Soc. Leather Technol. Chem.*, 2008, **92**, 81–84.
- 26 S. M. Olivannan and Y. Nayudamma, Studies in sulphonyl Chloride tannages (XI): reactions of sulphonyl chloride with modified proteins and model compounds, *Leather Sci.*, 1979, **26**, 54–61.
- 27 I. Chakarska, S. Todinova and K. Idakieva, Investigation on chemical cross-linked collagen phosphoric acid hydrolysates with cyanuric chloride by differential scanning calorimetry, *J. Therm. Anal. Calorim.*, 2010, **102**, 1–7.

